African Journal of Environmental Science and Technology Vol. 4(7), pp. 455-464, July 2010
Available online at http://www.academicjournals.org/AJEST
ISSN 1991-637X ©2010 Academic Journals

Full Length Research Paper

Delineating shallow ground water irrigated areas in the Atankwidi Watershed (Northern Ghana, Burkina Faso) using Quickbird 0.61 - 2.44 meter data

Gumma Murali Krishna[1]*, Thenkabail S. Prasad[2] and Barry Bubacar[3]

[1]International Rice Research Institute (IRRI), DAPO Box 7777, Metro Manila, Los Banos, Philippines.
[2]U.S. Geological Survey (USGS), Flagstaff, AZ 86001, USA.
[3]International Water Management Institute (IWMI), Ghana.

Accepted 28 April, 2010

The major goal of this research was to delineate the shallow groundwater irrigated areas (SGI) in the Atankwidi Watershed in the Volta River Basin of West Africa. Shallow ground water irrigation is carried out using very small dug-wells all along the river banks or shallow dug-outs all along the river bed. Each of these dug-wells and dug-outs are highly fragmented small water bodies that irrigate only a fraction of an acre. However, these are contiguous dug-wells and dug-outs that are hundreds or thousands in number. Very high spatial resolution (VHSR) Quickbird imagery (0.61 to 2.44 m) was used to identify: (a) dug-wells that hold small quantities of water in otherwise dry stream; and (b) dug-outs that are just a meter or two in depth but have dug-out soils that are dumped just next to each well. The Quickbird VHSR imagery was found ideal to detect numerous: (i) dug-wells through bright soils that lay next to each dug-well, and (ii) water bodies all along the dry stream bed. We used fusion of 0.61 m Quickbird panchromatic data with 2.44 Quickbird multispectral data to highlight SGI and delineate their boundaries. Once this was achieved, classification techniques using Quickbird imagery was used within the delineated areas to map SGI and other land use/land cover (LULC) areas. Results obtained showed that SGI is practiced on a land area of 387 ha (1.4%), rainfed areas is 15638 ha (54.7%) and the remaining area in other LULC. These results were verified using field-plot data which showed an accuracy of 92% with errors of omissions and commissions less than 10%.

Key words: Shallow groundwater, Quickbird, remote sensing, irrigated areas, Atankwidi Watershed, Ghana.

BACKGROUND AND RATIONALE

Land use and land cover studies involving the use of satellite image data require multispectral imagery from different seasons or dates and process methodologies used must be pixel oriented. Latest high resolution sensors, and others yet to come, together with the new existing data process environments, lead to important changes in the classification methodology (Manakos et al., 2000). High spatial resolution imagery gives more accurate information about the earth's surface. In African countries, it is generally difficult to map land use and land cover classes because there are no agriculture bunds in agriculture forms. Agriculture and other land use and land cover areas are very similar because of the nature of small-holder agriculture which is dominant in most parts of the continent. Image interpretation can be conducted digitally or visually. In case of high resolution images, interpretation depends on visual interpretation (Fijałkowska et al., 2005). Lewinski and Zaremski (2004) proposed the possible use of object-oriented classification and have shown that it results in impediment by the detailed information of the VHR images. Plantier et al. (2006) found that maximum likelihood technique could be applied for land use classification. However, the level of accuracy is low. In this study authors adopted methodologies from (Thenkabail et al., 2004; Gumma et al., 2009).

The importance and practice of the shallow ground water irrigation actually increases along the dryer river areas, since in these areas, the importance of dry season

*Corresponding author. E-mail: m.gumma@cgiar.org. Tel: +63 (2) 580-5600 ext: 2627, Fax: +63 (2) 580-5699.

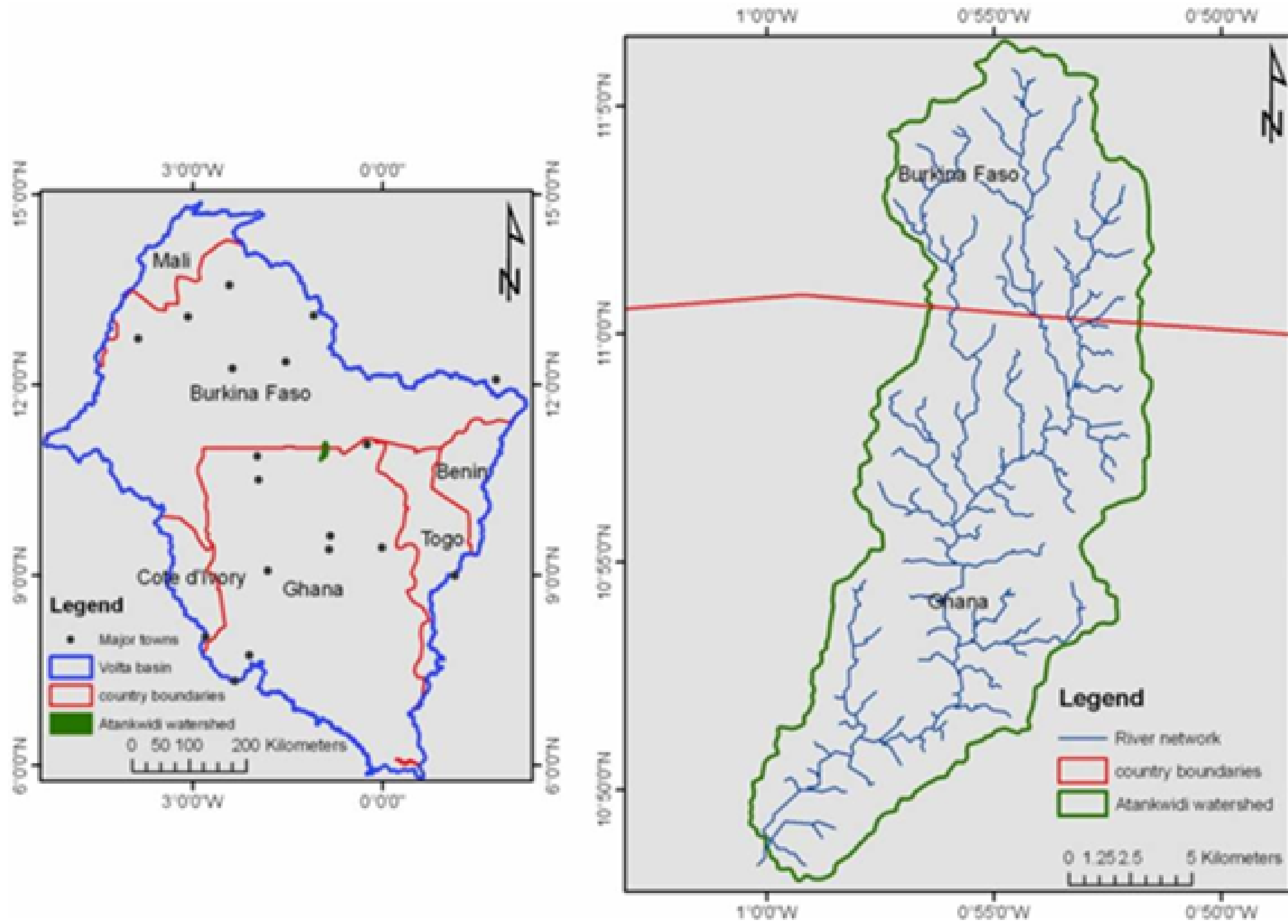

Figure 1. Volta basin with Atankwidi Watershed and its drainage network (extracted from SRTM DEM).

agriculture for increasing food production is a priority for agricultural development. Our current research efforts are directed at delineating the shallow groundwater irrigated areas in the Atankwidi Watershed including land use land cover and its methodologies.

The main objective of this project was to evaluate and map shallow groundwater irrigated areas and other land use and land cover based on intensive field plot data and high resolution imagery. The specific objectives of the project were to: (1) Delineate the shallow ground eater irrigated areas including land use land cover map using Quickbird data (08^{th} May 2008); (2) Conduct accuracy assessment using field plot data; and (3) Develop a methodology for delineating shallow ground water irrigated areas.

THE STUDY AREA

The Atankwidi is a tributary of the White Volta, flowing south from Burkina Faso into the Upper East Region of Ghana between Navrongo and Bolgatanga. The Atankwidi watershed (Figure 1), 276 km^2 in area, is typical of agricultural catchments found in the Upper East Region, which is situated between the northern Guinea and the Sudan savanna zones. Within the transition zone, vegetation is characterized by open woodland savannas associated with perennial grasses in the south, and increasingly with annual tussock grasses in the northern zone (Iloege, 1980; Windmeijer and Riesse, 1993). Annual precipitation is around 990mm distributed over pronounced rainy (April to October) and dry (October to March) seasons, and annual average temperatures are above 18°C (Martin, 2005).

The Soil Research Institute of Ghana distinguishes three main soil types in the catchment (Environmental Protection Agency / World Bank, 1999). These are: (1) Leptosols, which are predominant along the elevated northern and eastern border; (2) Fluvisols, which are found in the flat terrain to the sides of the main stream, and (3) Lixisols, which covers the rest of the catchment. The hydrogeology and climatic conditions of the catchment are typical for a large part of the Volta River basin. Thus the results of studies conducted in this catchment are transferable to other areas of the basin. The Antankwidi catchment is one of the areas with the

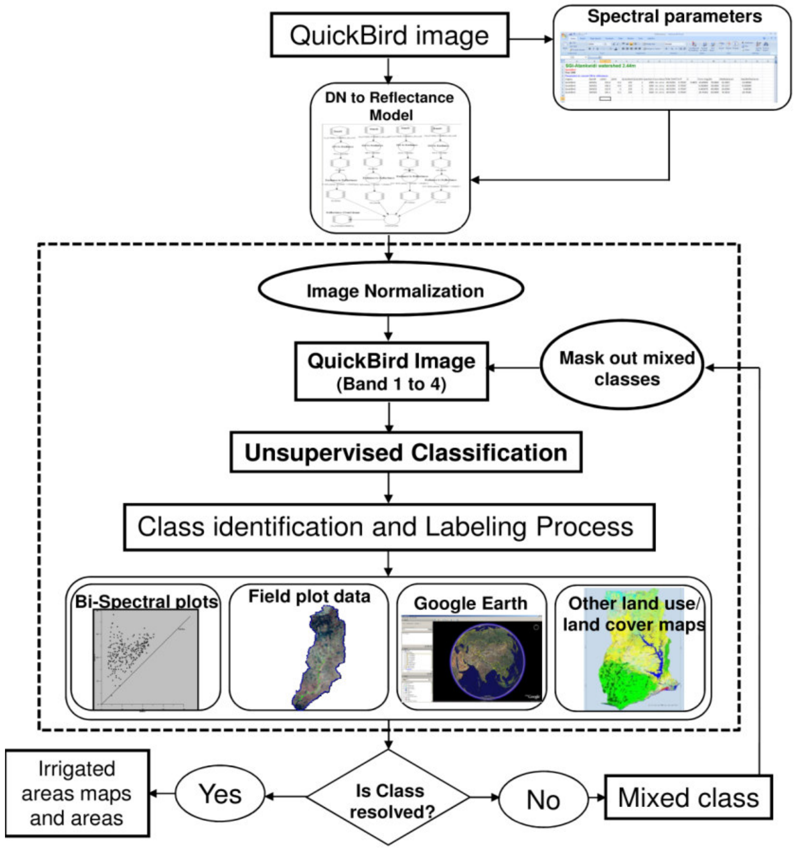

Figure 2. Methodology flow chart showing approach used to delineate shallow ground water irrigated areas (SGI) from other land use\land cover (LULC) areas.

highest groundwater use per km^2 in the Volta River Basin (Martin, 2006). The main aquifer is the regolith aquifer in the weathered zone of granitoids. This hydrogeology is typical for about two thirds of the area of the Volta River basin, which are underlain by Birimian rocks. More than 80 % of all boreholes in the basin target the weathered rock aquifer. Hydrological conditions in the study area are therefore representative for the main groundwater resources in the basin.

METHODOLOGY

Land use changes were investigated using Quick Bird images for year 2008. An overview of the methods and analytical techniques are shown in Figure 2. Briefly, the process involved the Normalization of each of the four bands in the Quick Bird imagery using the reflectance model (Gumma et al., 2009). Quick Bird image was then classified using unsupervised ISOCLASS cluster K-means classification (reference).

Bi-spectral plots that represent each unsupervised class in two-dimensional feature space were then generated using the red and near infrared bands (band 3 and band 4). Class identification and labeling was based on these bi-spectral plots, as well as ground truth data and very high resolution images (from Google Earth). The grouping of these classes was based on spectra l signatures, large volumes of ground truth data and the use of very high resolution imagery. Mixed classes were resolved through the inclusion of relevant spatial data (such as elevation and rainfall), and establishing methods for irrigated area calculations and accuracy assessments.

Image normalization

Satellite sensor data

The Quickbird imagery was purchased through Landsat Science Team allocations. The characteristics of this image are shown in Table 1. The image was converted into at-sensor reflectance based on the equations and algorithms presented in (Markham and Barker (1986), Thenkabail et al. (2004). The Quickbird data (Table 1) were used as the primary data source for delineating shallow groundwater irrigated areas in the watershed.

Quickbird data to radiance

The radiometric resolution of Quickbird imagery is 11-bit and stored in 16-bit. There are two steps to calculate radiance from digital number. Quickbird DNs were converted to radiance (m W cm^{-2} sr^{-1}) using the equation

$$L_{ij} = DN_{ij} * [CalCoef_j]^{-1} , \quad (1)$$

Table 1. Characteristics of satellite sensor data used in the study.

Sensor	Spatial (meters)	Spectral (#)	Radiometric (bit)	Band range (μm)	Irradiance ($W\ m^{-2} sr^{-1}\ \mu m^{-1}$)	Sun elevation θ	Earth sun distance D	Data points (#per hectares)
QUICKBIRD	0.61-2.44	4	11	0.45 - 0.52	1381.79	68.23	1.0005	10000, 625
				0.52 - 0.60	1924.59			
				0.63 - 0.69	1843.08			
				0.76 – 0.89	1574.77			

Figure 3. Field-plot data showing dug-wells and dug-outs.

where L_{ij} and DN_{ij} are the in-band radiance at sensor aperture (mW cm^{-2}-sr^{-1}) and image product digital value of the i^{th} pixel in the j^{th} band, respectively, and $CalCoef_j$ is the in-band radiance calibration coefficient (DN $cm^{2*}sr\ m^{-1}W^{-1}$). Since the Quickbird image used in this study was acquired after February 22, 2001, the values of $CalCoef_k$ factor as 0.064 for Pan band, 0.016 for blue, 0.014 for green, 0.013 for red and 0.015 for NIR.

Radiance to reflectance

A reduction in between-scene variability can be achieved through a normalization for solar irradiance by converting spectral radiance, as calculated above, to planetary reflectance or albedo (Markham and Barker, 1985; 1987). This combined surface and atmospheric reflectance of the Earth is computed with the following formula:

$$\rho_p = \frac{\pi L_\lambda d^2}{ESUN_\lambda \cos\theta_S} \quad (2)$$

where ρ_p is the at-satellite exo-atmospheric reflectance, L_λ is the radiance (W m^{-2} sr^{-1} μm^{-1}), d is the earth to sun distance in astronomic units at the acquisition date (see Markham and Barker, 1986), $ESUN_\lambda$ is the mean solar exo-atmospheric irradiance (W m^{-2} sr^{-1} μm^{-1}) or solar flux (Neckel and Labs, 1984), and θ_S is solar zenith angle in degrees (that is, 90 degrees minus the sun elevation or sun angle when the scene was recorded as given in the image header file).

Field-plot datasets

Field-plot data was collected between June 3rd -13th, 2008 for 190 sample sites (Figure 4) covering major irrigated areas (which includes shallow dug wells and dug outs in riverbed) along the river, rainfed fallows and other land use land cover classes and its percents in the watershed. In addition, ground truth observations were made extensively, while driving, by capturing other few more locations for additional information in class identification.

The Landsat data requires a minimum sampling unit (which is suitable for <30 m resolution like IKONOS, Quickbird etc) of 30 x 30 m for ground truth validation. The approach we adopted was to look for contiguous areas of homogeneous classes within which we can sample. A large contiguous information class constituted our sampling unit, within which we sample a representative area of 30 by 30 m. The emphasis was on “representativeness” of the sample location in representing one of the classes to ensure precise geolocation of the pixel. Class labels were assigned in the field. Classes have the flexibility to merge to a higher class or break into a distinct class based on the land cover percentages observed at each location. The precise locations of the samples were recorded by a Garmin GPS unit. The sample size varied from 10 - 40 samples for each category, and also at each location we captured two to three photographs (Figure 3). At each location the following data were recorded (e.g):

1. GT Site no
2. Coordinates (Using GPS)
3. Topographic position
4. Agriculture technique (Rainfed, Irrigated: dryseason, and etc)
5. Irrigation techniques \ watering methods: Ex;

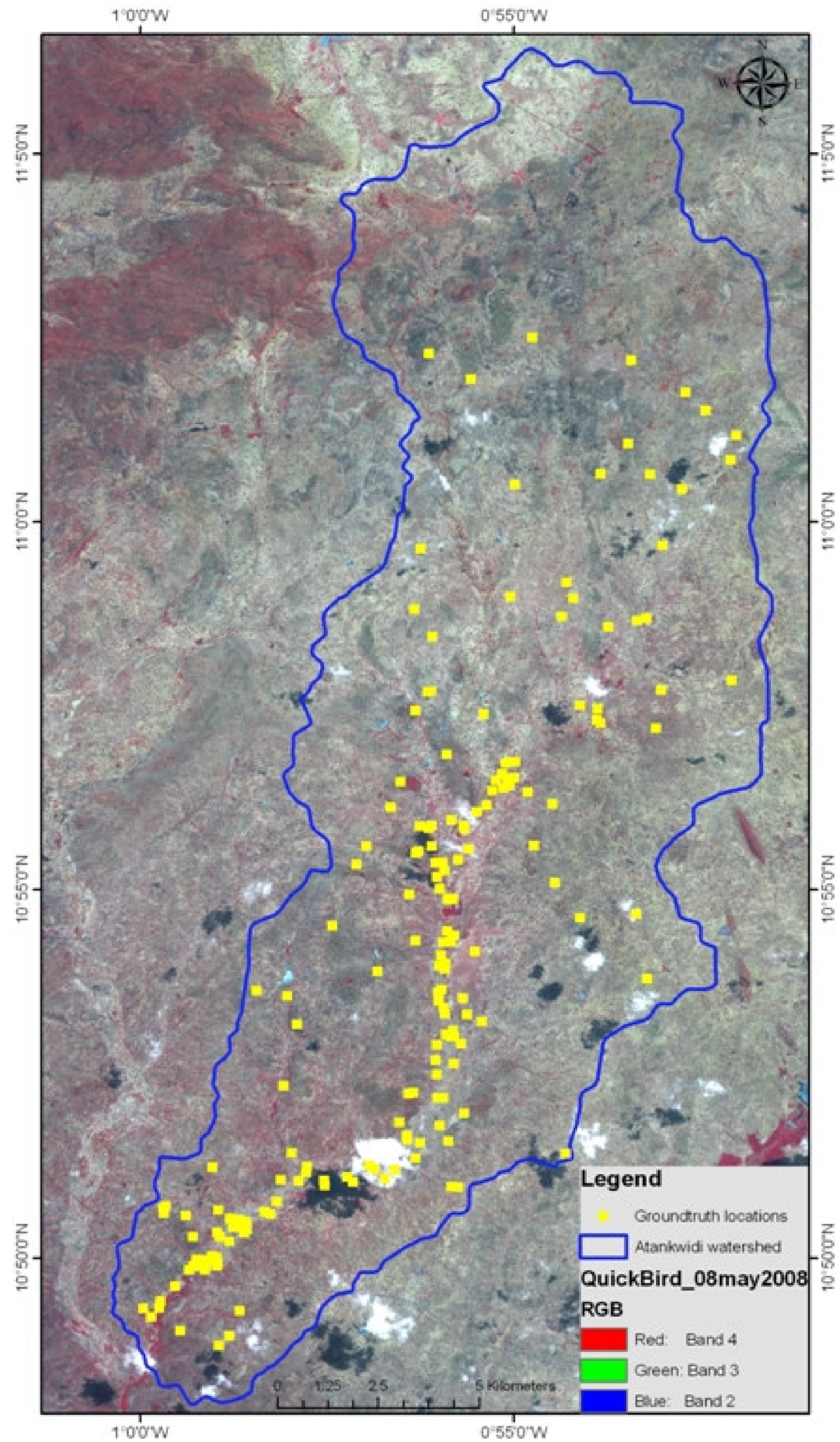

Figure 4. Location of ground-truth sampling sites in the Atankwidi Watershed over laid on QuickBird imagery.

a. Dug well irrigated areas during dry season
b. Dug out irrigated areas during dry season
c. Combined dug well and dug out irrigated areas during dry season

9. Fringe length and bottom width
10. Shape of the valley
11. Soil moisture
12. Land use/land cover (LULC) classes
13. Land cover types (% cover): trees, shrubs, grasses, barren land/soil, rock, water, built-up, farmland, and others.
14. Crop grown on farm land: for summer seasons and rainy season, Ex: Cassava/Yam, Cocoa, Vegetables/Fruits, Sorghum/ Maize, Banana, Rice, Barren Farmland, Plantations and others.

435 Digital photos hot linked at 190 locations

The data were organized in Arc view 3.2a, Arc Map, ARC Info 9.1 and ERDAS Imagine 9.1 compatible formats with accompanying metadata so as to spatially locate them over the QuickBird image data precisely (Figure 4).

Unsupervised classification

Unsupervised classification using ISOCLASS cluster algorithm (ISODATA in ERDAS Imagine 9.2TM) followed by progressive generalization (Cihlar et al., 1998) was used to classify the data. With a maximum of 40 iterations and convergence threshold of 0.99, 40 classes were generated. Use of unsupervised techniques is recommended for large areas that cover a wide and unknown range of vegetation types, and where landscape heterogeneity complicates identification of homogeneous training sites (Achard et al., 1995; Cihlar, 2000).

The 40 classes obtained from the unsupervised classification were merged using bi-spectral plots, intensive ground truth data (described below), and Google earth imagery (Gumma et al., 2009; Thenkabail et al., 2005; Tucker et al., 2005). For cloud patches we used old data sets (06th February 2008).

Class identification and labeling process

Class identification and labeling is based on Bispectral plots, ground truth data and Google earth imagery.

Bi-spectral plots

The spectral properties of the classes obtained through unsupervised classification were performed on the megafile using ISODATA statistical cluster algorithm for multi dimensional data (ERDAS, 2008). The Bi-spectral plot for all classes was obtained by plotting the spectral reflectance of Band 3, Red (Quickbird), on X Axis and spectral reflectance of Band 4, Near Infrared (Quickbird), on Y Axis (Figure 5). The diagonal line in the graph represents the soil line. The Soil line clearly separates the classes with vegetation above the soil line from the classes without vegetation below the Line. The classes with similar spectral reflectance fall nearby as a cluster such classes may represent same category with a slight variation in reflection. These classes like water bodies and forest with large variation in Vegetation can be easily identified and labeled.

Ground truth datasets

Ground-truth data was collected between June 3rd -13th, 2008 for 190 sample sites covering major irrigated areas (which includes shallow dug wells and dug outs in riverbed) along the river, rainfed fallows and other land use land cover classes and its percents in the watershed. In addition, ground truth observations were made extensively, while driving, by capturing other few more locations for additional information in class identification.

The precise locations of the samples were recorded by a Garmin GPS unit. The sample size varied from 10-40 samples for each category, and also each location we captured two to three photo graphs. These groundtruth data and associated photographs were used in class identification and labeling process.

Google earth data

Google Earth (http://earth.google.com/) contains increasingly comprehensive image coverage of the globe at very high resolution 0.61 - 4m, with different seasonal images. In this study, Google Earth data were used for: a) Identification and labeling of classes (cloud affected areas), b) accuracy assessment of irrigated areas and c) finally the classified output overlay on Google Earth to verify the classes.

Resolving mixed classes

Some classes were locally misclassified and intermixed with neighboring classes and such misclassified pixels were normally identifiable using groundtruth data points where land use types were mapped out of their normal context (Fuller et al., 1998). For example, the class “fallow” mix with “rangelands”. Such misclassification could be removed by contextual correction methods (Groom et al., 1996; Thenkabail et al., 2006). These mixed classes separate out from the classification and masking the original image and then reclassified in to 10 classes to separate mix classes. Based on the above procedure, identified classes were with the base classified map.

Accuracy assessment

The accuracy assessment was carried out using (Congalton and Green, 1999) as follows:

$$\text{Accuracy of irrigated area class} = \frac{\text{Field-ploted irrigated points classified as irrigated area}}{\text{Total number of field-ploted points of irrigated area class}} \times 100$$

$$\text{Errors of commission for irrigated area class} = \frac{\text{Non-Irrigated field-plot points classified as irrigated area}}{\text{Total number of non-irrigated field-plot points}} \times 100$$

$$\text{Errors of commission for irrigated area class} = \frac{\text{Irrigated field-plot points falling on nonirrigated area class}}{\text{Total number of field-ploted points of irriated area class}} \times 100$$

RESULTS AND DISCUSSION

Land use / land cover maps

The unsupervised classification based on the ISODATA

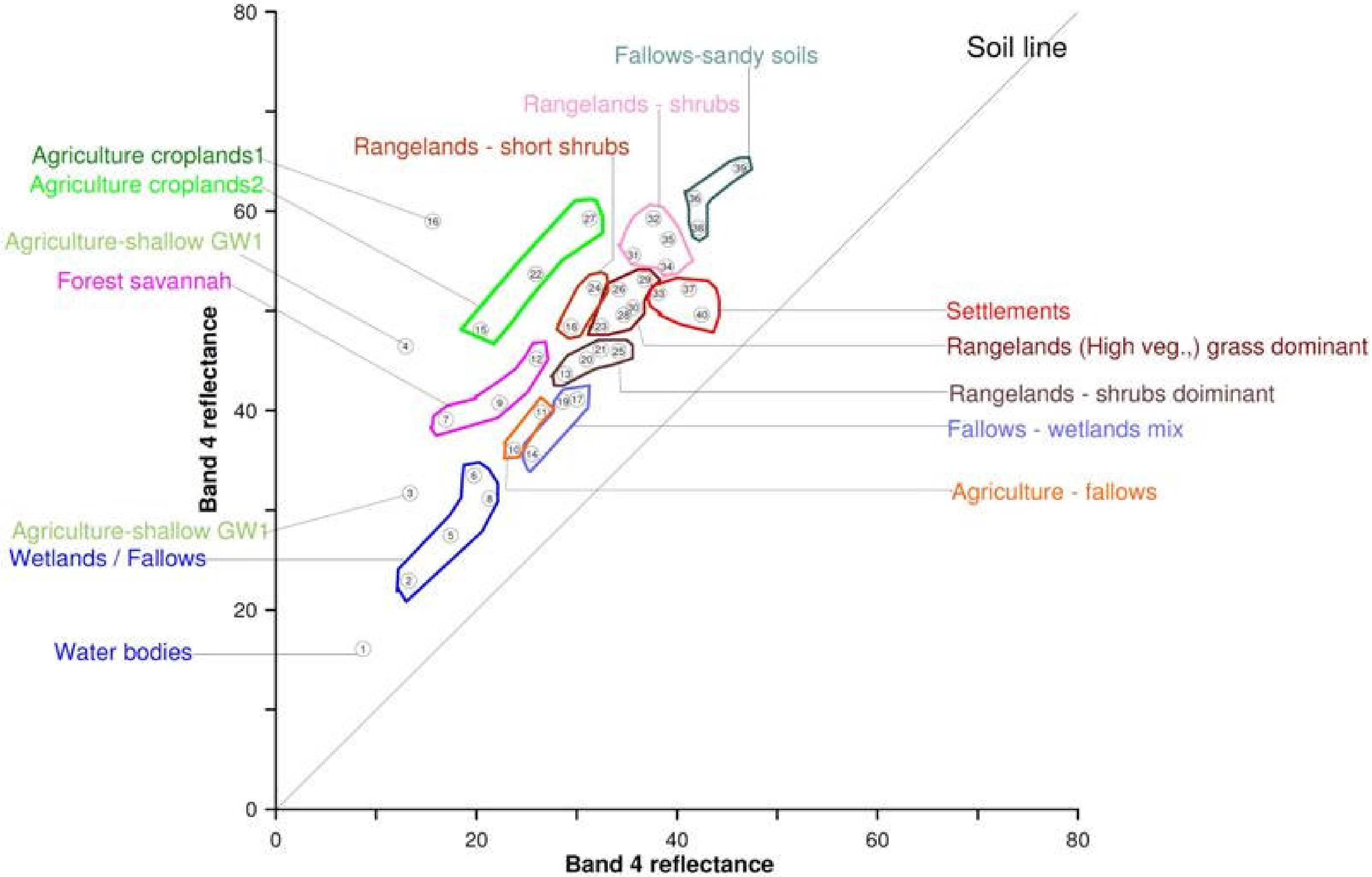

Figure 5. Bi-spectral plot to separate shallow ground water irrigated areas from other land use\land cover (LULC) areas.

clusters was done initially by obtaining 40 classes. Mixed classes were re-classified into 10 classes, thus, resulting in a total of 50 classes. These were, then, grouped into 14 broad classes which were mapped to show clear spectral separability (Figure 6). Classes identified based on field-plot data includes GPS referenced digital images and field observations. The land use land cover (LULC) areas in the watershed were shown in the Table 2. More than a third of the basin is rangeland-rainfed fallows (40%). Rainfed agriculture is by fare the most dominant production system in the Atankwidi basin and irrigation is relatively limited only 0.1% in terms of area but well spread out in the Ghana portion of the watershed. In the Burkina side there is no SGI.

Accuracy assessment

A qualitative accuracy assessment was performed to check if the shallow groundwater irrigated areas are classified as irrigated or not, without checking for crop type or type of irrigation. The accuracy assessment was performed using field-plot data, to derive robust understanding of the accuracies of the datasets used in this study. The field-plot data was based on an extensive field campaign conducted throughout Atankwidi Watershed during dry season by International Water Management Institute researchers and consisted of 190 points. Accuracies are varying from 61 to 100%. Barren lands are less accurate because it spreading up stream watershed and mix with rangelands. Accuracy assessment provides realistic class accuracies (see equations above) where land cover is heterogeneous and pixel sizes exceed the size of uniform land cover units (Gopal et al., 1994, Thenkabail et al., 2005; Gumma et al., 2009). For this study we had assigned 3 x 3 cells of QuickBird pixels around each of the field-plot points to one of six categories : absolutely correct (100% correct), mostly correct (75 % or more correct), correct (50% or more correct), incorrect (50% or more incorrect), mostly incorrect (75% or more incorrect), and absolutely incorrect (100% incorrect). Class areas were tabulated for a 3 x 3-pixel (9 pixels) window around each field-plot point. If 14 out of 14 QuickBird classes matched with field-plot data, then it was labeled according to the six categories defined. The accuracy assessments patterns are presented in Table 3. This data shows that use of remote and high image resolution can be very accurate

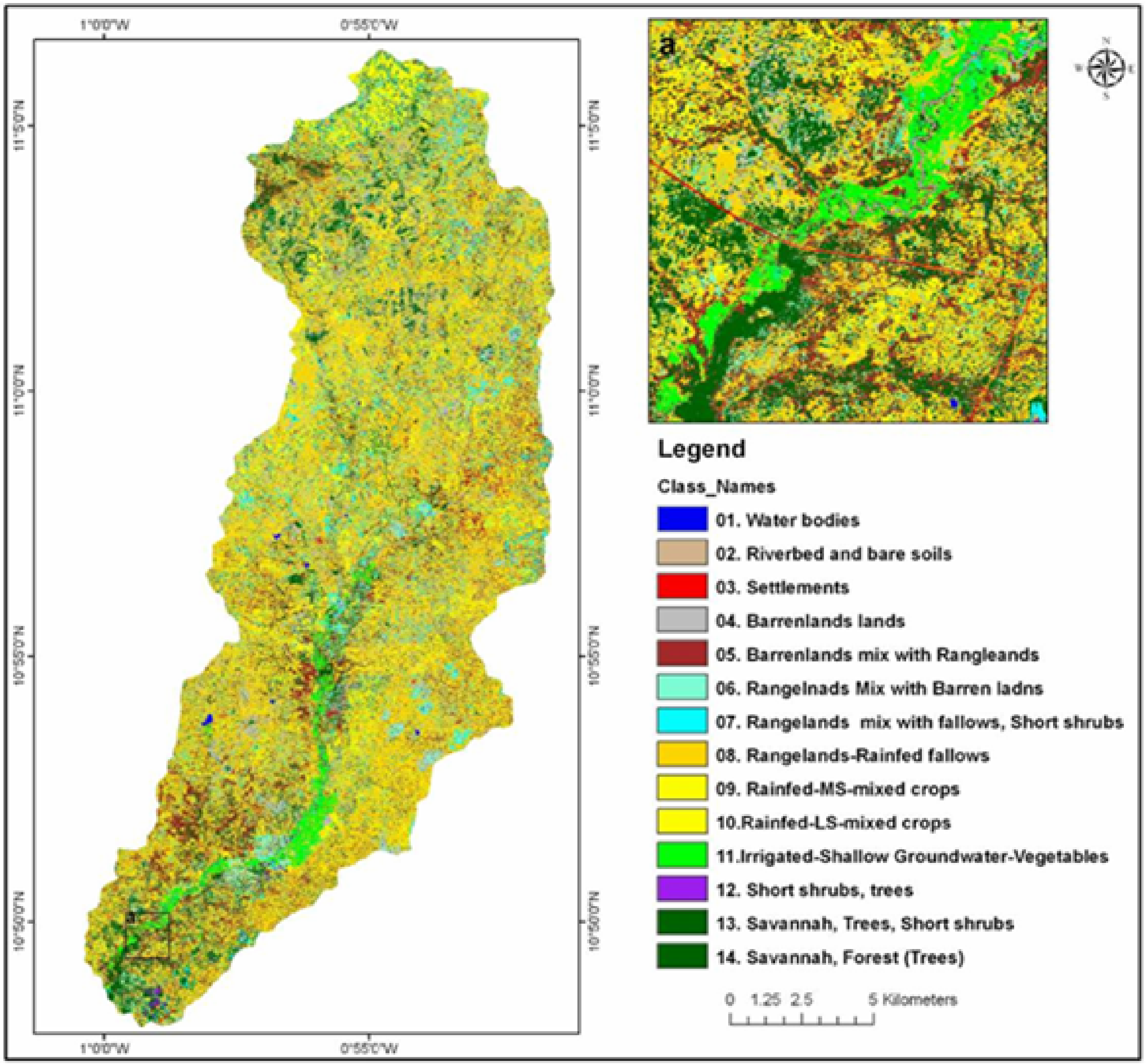

Figure 6. The shallow ground water irrigated areas (class 11) along the stream course in the Atankwidi watershed. Clear delineation of SGI from other areas is apparent.

Table 2. Land use / land cover areas and its percentages.

S/No.	Land use/Land cover	Area (Ha)	% area
1	Water bodies	31.82	0.1
2	Riverbed and bare soils	116.58	0.4
3	Settlements	104.96	0.4
4	Barren lands	3014.16	10.5
5	Barrenlands mix with rangelands	2852.02	10.0
6	Rangelands Mix with Barren lands	873.19	3.0
7	Rangelands mix with fallows, Short shrubs	2079.77	7.3
8	Rangelands-rainfed fallows	11410.77	39.9
9	Rainfed-MS-mixed crops	1712.45	6.0
10	Rainfed-LS-mixed crops	2515.59	8.8
11	Irrigated-shallow groundwater-vegetables	387.23	1.4
12	Short shrubs, trees	64.42	0.2
13	Savannah, trees, short shrubs	1578.62	5.5
14	Savannah, forest (Trees)	1891.07	6.6
		28632.62	100.0

Table 3. Accuracy assessment based on field-plots.

Lulc #	Samples #	Total correct	Absolute correct	Mostly correct	Correct	Incorrect	Mostly incorrect	Absolute correct	Total incorrect
01. Water bodies	0	100	1.0	0.0	0.0	0.0	0.0	0.0	0
02. Riverbed and bare soils	1	100	1.0	0.0	0.0	0.0	0.0	0.0	0
03. Settlements	0	100	1.0	0.0	0.0	0.0	0.0	0.0	1
04. Barrenlands lands	18	61	0.2	0.0	0.4	0.4	0.0	0.0	39
05. Barrenlands mix with Rangelands	10	80	0.6	0.0	0.2	0.2	0.0	0.0	20
06. Rangelands Mix with Barren lands	4	81	0.3	0.0	0.6	0.2	0.0	0.0	19
07. Rangelands mix with fallows, Short shrubs	11	88	0.8	0.0	0.1	0.1	0.0	0.0	13
08. Rangelands-rainfed fallows	35	100	1.0	0.0	0.0	0.0	0.0	0.0	0
09. Rainfed-MS-mixed crops	14	100	1.0	0.0	0.0	0.0	0.0	0.0	0
10.Rainfed-LS-mixed crops	12	92	0.8	0.0	0.1	0.1	0.0	0.0	8
11.Irrigated-shallow groundwater-vegetables	70	94	0.9	0.0	0.0	0.0	0.0	0.0	6
12. Short shrubs, trees	5	100	1.0	0.0	0.0	0.0	0.0	0.0	0
13. Savannah, trees, short shrubs	6	94	0.9	0.0	0.0	0.0	0.0	0.0	6
14. Savannah, forest (Trees)	4	100	1.0	0.0	0.0	0.0	0.0	0.0	0
	190	92	0.8	0.0	0.1	0.1	0.0	0.0	8

Absolutely correct: 100% correct; Mostly correct: 75% or more correct; Correct: 50% or more correct; Incorrect: 50% or more incorrect; Mostly incorrect: 75% or more incorrect; and absolutely incorrect: 100% incorrect.

in assessing the extent of SGI in the White Volta Basin.

Conclusion

The paper demonstrated the strength of using very high spatial resolution (VHSR) Quickbird imagery of 0.61 - 2.44 m spatial resolution to highlight, delineate, and map shallow ground water irrigated areas (SGI). The method was demonstrated for Atankwidi Watershed (Northern Ghana) which has very small sub-acre plots of irrigated areas from dug-wells and dug-outs. However, these small dug-outs irrigating sub-acre plots are numerous and contiguous all along the stream bank. Similarly, the dug-outs are numerous small water bodies all along the dry stream beds. The quickbird 0.61 to 2.44 m imagery was fused to highlight and delineate these contiguous areas of dug-wells and dug outs. Once the areas are delineated, classification techniques were used on the delineated areas using quickbird imagery to identify and map SGI and other LULC areas.

ACKNOWLEDGEMENTS

The authors acknowledge International Water Management Institute for providing necessary facilities and infrastructure. We also thank Simon, Daniel and Jacob for intensive help during the field visit. First author would like to thank Dr. Paul Pavelic, Senior Researcher, IWMI-Hyderabad, who was encouraging and supporting throughout research, and NASA for providing high resolution imagery.

REFERENCES

Achard F, Estreguil C (1995), Forest classification of Southeast Asia using NOAA AVHRR data. Remote Sensing Environ., 54: 198- 208.
Cihlar J, Xiao Q, Beaubien J, Fung K, Latifovic, R (1998), Classification by progressive generalization: a new automated methodology for remote sensing multichannel data. Int. J. Remote Sensing, 19: 2685-2704.
Cihlar J (2000). Land cover mapping of large areas from satellites: status and research priorities. Int. J. Remote Sensing, 21: 1093-1114.
Congalton RG, Green K (1999). Assessing the accuracy of remotely sensed data: principles and practices. New York: Lewis.
Fijałkowska A, Chmiel J, Kupidura P, Pluto-Kossakowska J, Zieliński R (2005). Land Use discrimination of agricultural parcels Using spring vhr satellite image data. 11th Conference on Control with Remote Sensing of area-based subsidies 23th - 25th November 2005 Kraków (POLAND).
Fuller RM, Groom GB, Mugisha S, Ipulet P, Pomeroy D, Katende A, Bailey R, Ogutu-Ohwayo R (1998). The integration of field survey and remote sensing for biodiversity assessment: a case study in tropical forests and wetlands of Sango bay, Uganda. Biol. Conserv., 86: 379-391.
Gopal S, Woodcock CE (1994). Theory and Methods for Accuracy Assessment of Thematic Maps Using Fuzzy Sets, Photogram. Engine. Remote Sensing, 60(2): 181-188.
Groom GB, Fuller RM, Jones AR (1996). Contextual correction: techniques for improving land cover mapping from remotely sensed images. Int. J. Remotesen., 17: 69-89.
Gumma MK, Thenkabail PS, GangadharaRao TP, Nalan SA, Velpuri NM, Biradar C (2009). Agriculture Cropland Change Response to Water availability using Spectral Matching Techniques in the Krishna River Basin (India). Int. J. Remote Sensing, TRES-PAP-2009-0162. (Press)
Lewinski S, Zarenski K (2004) Examples of object-oriented classification performed on high-resolution satelite images. Miscellanea Geographica. 11: 349-358.
Manakos I, Scheneider T, Ammer U (2000). A Comparison Between the ISODATA and the eCognition Classification Methods on Basis of Field Data. IAPRS, 33(Supp. B7): 133-139.
Markham BL, Barker JL (1986). Landsat MSS and TM Post-Calibration Dynamic Ranges, Exoatmospheric Reflectances and At-Satellite Temperatures, Earth Observation Satellite Co., Lanham, MD, Landsat Technical Notes.
Martin N (2005). Development of a Water Balance for the Atankwidi Catchment, West Africa—A Case Study of Groundwater Recharge in a Semi-Arid Climate. Doctoral Thesis, University of Go¨ ttingen, Germany, p. 176
Plantier TM, Loureiro P, Marque MC (2006). Spectral analyses and classification of ikonos images for forest cover characterisation. Proceedings of the 2nd Workshop of the EARSeL SIG on Land Use and Land Cover, Center for Remote Sensing of Land Surfaces, Bonn, 28-30.
Thenkabail PS, Enclona EA, Ashton MS (2004). Hyperion, IKONOS, ALI, ETM+ sensors in the study of African rainforests, Remote Sensing Environ., 90: 23-43.
Thenkabail PS, Schull M, Turral H (2005). Ganges and Indus River Basin Lan Use/Land Cover (LULC) and irrigated area Mapping using Continuous Streams of MODIS Data. Remote Sensing Environ., 95(3): 317-341.
Neckel H, Labs D (1984). The solar radiation between 3300 and 12500 A. Solar Phys., 90: 205-258
Tucker CJ, Grant DM, Dykstra JD (2005). NASA's global orthorectified Landsat data set. Photogram. Engine. Remote Sensing, 70: 313-322.